ELSEVIER

Chemical Engineering Journal 123 (2006) 81–91

Chemical Engineering Journal

www.elsevier.com/locate/cej

A new liquid distribution factor and local mass transfer coefficient in a random packed bed

T. Dang-Vu, H.D. Doan *, A. Lohi, Y. Zhu

Department of Chemical Engineering, Ryerson University, 350 Victoria Street, Toronto, Ontario M5B 2K3, Canada

Received 1 March 2006; received in revised form 24 July 2006; accepted 31 July 2006

Abstract

Liquid distribution and local mass transfer in a packed bed of 25.4 mm metallic Pall rings were investigated. The liquid collecting method and electrochemical technique were used to measure local liquid flow rates and local mass transfer coefficients, respectively. Measurements were carried out at various radial and axial positions in the bed at varied liquid flow rates with three different liquid distributor designs: single point (SLD), cross (CLD), and ladder type (LLD) distributors. A new liquid-distribution factor for the liquid flow pattern in a packed bed was proposed and used for evaluation of liquid distribution in the bed. Liquid distribution and the local mass transfer coefficient for SLD were more sensitive to the bed height than those for CLD and LLD, as expected. Liquid redistribution was observed at x/D (the ratio of the packing height to the tower diameter) level of 4.9. The effect of the inlet liquid flow rate on local mass transfer was found to be significant for all liquid distributors. Local mass transfer coefficient increased with the inlet liquid flow rate. A correlation of the overall mass transfer with the particle Reynolds number was also developed taking into account the volume segments of different radial and axial regions in the bed. The mass transfer coefficient, in terms of the Sherwood number, was found to be proportional to the Reynolds number to a power of 0.26 for CLD and 0.44 for SLD.

Keywords: Liquid distribution; Local mass transfer; Limiting current; Distribution factor

1. Introduction

A packed bed is one of the most common unit operations applied for interphase transport in chemical industries. This has prompted extensive studies of mathematical and physical model for these systems. Consequently, there exists a large number of publications on liquid distribution in the packed column using different techniques from the simple liquid collecting method [1,2] to the more advanced techniques, such as: tracing method [3,4], conductance probe [5,6], and tomographic measurement [7–9].

The liquid collecting method has been used widely to investigate liquid distribution in a packed column due to its simplicity in measurements as well as data analyses [1,2,10–16]. This method is based on the collection of liquid flowing down into a special vessel at the outlet of the bed. In this vessel, liquid is collected in an array of cells or concentric cylinders and then the liquid volume is measured versus time. Local liquid velocity is usually used to quantify the liquid distribution in a packed bed, and various mathematical models have been developed for liquid flow distribution. Some of the typical models are shown below.

Groenhof [10] defined the liquid maldistribution index, M_{f1}, as a root mean square deviation of f_{ij} values from their mean f_{av} as follows:

$$M_{f1} = \sqrt{\sum_i \sum_j \frac{(f_{ij} - f_{av})^2}{n}} \quad (1)$$

where i is the ordinal number of a collecting cell, j the ordinal number of an experiment, f_{ij} the ratio of the measured liquid flow rate into a collecting cell to the flow rate expected for a perfectly uniform liquid distribution, n is the number of f_{ij} values.

One of the most fundamental studies on liquid distribution in a packed column is that of Hoek et al. [1]. In their study the effects of a wide variety of factors including packing characteristics (type, size, and packing height), liquid distributors, and operational conditions (e.g. liquid flow rates) on the liquid distribution were investigated. The maldistribution factor M_{f2} was defined as the square of the relative standard deviation of the

* Corresponding author. Tel.: +1 416 979 5000x6341; fax: +1 416 979 5083.
E-mail address: hdoan@ryerson.ca (H.D. Doan).

1385-8947/$ – see front matter © 2006 Elsevier B.V. All rights reserved.
doi:10.1016/j.cej.2006.07.013

Nomenclature

a	cathode surface area (m^2)
A	area of the column cross-section (m^2)
A_i	area of the ith collecting section (m^2)
A_s	area of the local segment around a measuring point (m^2)
C_∞	bulk concentration of ferricyanide (mol m^{-3})
d_p	equivalent diameter of packing (m)
D_e	diffusion coefficient of ferricyanide in solution ($m^2\ s^{-1}$)
D_L	liquid distribution factor
F	Faraday constant (96,487 C mol^{-1})
F_a	area factor ($F_a = A_s/A$)
F_h	height factor ($F_h = H_s/H$)
F_v	volume factor ($F_v = F_a F_h$)
G	gas flow rate (kg $m^{-2}\ s^{-1}$)
H	overall packing height in the column (m)
H_s	length of a segment in the axial direction (m)
i_L	limiting current for ferricyanide reduction (A)
k_{L-S}	liquid-phase mass transfer coefficient of ferricyanide at solution/packing interface (m s^{-1})
L_{av}	average volumetric flow rate for all collectors in column ($m^3\ s^{-1}$)
L_i	volumetric flow rate to ith collector in column ($m^3\ s^{-1}$)
M_f	liquid maldistribution factor
n	total number of collectors or sampling electrodes in column
r/R	dimensionless radial distance from the center of bed cross-section
Re	Reynolds number, $Re = \frac{Ud_p\rho}{\mu}$
Sc	Schmidt number, $Sc = \frac{\mu}{\rho D_e}$
Sh	Sherwood number, $Sh = \frac{k_L d_p}{D_e}$
U	superficial velocity of liquid (m s^{-1})
x/D	dimensionless axial distance from liquid distributor
z	number of electron transferred during reduction of each ferricyanide ion

Greek letters

μ	kinematic viscosity ($m^2\ s^{-1}$)
ρ	density (kg m^{-3})

flow distribution as follows:

$$M_{f2} = \frac{1}{n}\sum_{i=1}^{n}\left(1 - \frac{L_i}{L_{av}}\right)^2 \quad (2)$$

where L_i is the liquid flow rate to the collecting cell ith, and L_{av} is the average liquid flow rate.

The liquid maldistribution factor was redefined by Kouri and Sohlo [2] taking into account the areas of the collecting cells and the column:

$$M_{f3} = \sqrt{\sum_{i=1}^{n}\frac{A_i}{A}\left(1 - \frac{L_i}{L_{av}}\right)^2} \quad (3)$$

where A_i is the area of the ith annular collecting section, A the cross-sectional area of the column, L_i the liquid flow rate to the ith annular section and L_{av} is the average liquid flow rate over the column cross-section.

Several maldistribution factors have been proposed and reported in the literature. However, from mathematical point of view, these factors show only the deviation of individual (local) measured values from the average of all measured values; hence, they do not represent the deviation of individual measured values from the values under an ideal condition, i.e. the local liquid flow rate when liquid distribution is ideally uniform in a packed bed. In addition, they do not show clearly the development of the liquid flow pattern in the bed. For example, when the local liquid flow rates at individual measuring points are comparable among themselves, the calculated maldistribution factor would be low, indicating good liquid distribution. However, liquid flow distribution in the bed might be still far from uniformity since the measured values may differ (larger or smaller) from the actual liquid flow rate.

Mass transfer in a packed column has also been extensively investigated. Various methods have been used in those studies, such as: dissolution [17–19], electrochemical [20,21], and gas absorption [22,23]. Through these methods, the effect of a variety of factors namely packing characteristics (type, size, and packing height), initial liquid distribution, and fluid flow rate on the mass transfer coefficient was investigated. Many mathematical models for mass transfer in a packed bed have been proposed. However, direct measurements of the local mass transfer coefficient in a packed bed was only done in our earlier study using the electrochemical technique [20], and a mathematical model for local mass transfer coefficient in a packed bed was proposed recently [21]. This model allows predictions of the local mass transfer coefficient at any axial and radial positions in the packed bed of metal Pall rings.

Although liquid distribution and mass transfer in a packed column have been studied by several researchers, they were usually reported as separate works. It is well known that liquid distribution directly affects mass transfer in a packed bed. The present study is an extension of our previous work [15,20,21] on investigation of the influence of liquid distribution on mass transfer in a packed bed. The effects of initial liquid distribution, the packing height, and liquid and gas flow rates on liquid distribution and local mass transfer coefficient were investigated.

2. Methodology

2.1. Experimental set-up

The experimental apparatus consists of a 0.3 m diameter PVC column filled with 25.4 mm stainless steel Pall rings to 2.1 m height as shown in Fig. 1. Two different configurations of

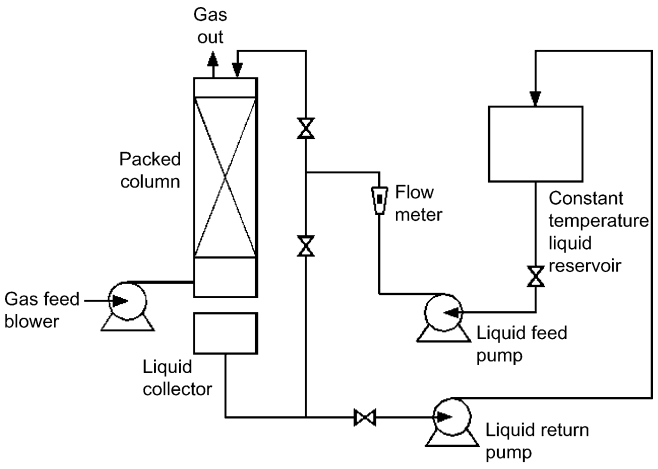

Fig. 1. Schematic diagram of the experimental setup.

experimental system were used for liquid distribution and mass transfer coefficient measurements.

For liquid distribution measurements, the liquid collecting method was used with air–water system. The liquid flow rate was varied from 2.6 to 7.8 kg m^{-2} s^{-1}. Two gas flow conditions (0 and 0.9 kg m^{-2} s^{-1}) were used to study the effect of the gas flow rate on liquid distribution. Liquid flowing down the bed was collected in a collector with 39 tubes of 25.4-mm diameter. The tubes were arranged circularly at four different radial positions as shown in Fig. 2. Measurements were carried out at four axial levels from the top of the packing: 0.5, 1.0, 1.5, and 2.0 m. These axial levels are equivalent to the ratios of the axial distance from the top of the packed bed to the tower diameter, x/D, of 1.6, 3.3, 4.9, and 6.6. The wall flow was separated from the bulk flow in the packing by an annular ring on the inside wall of the column

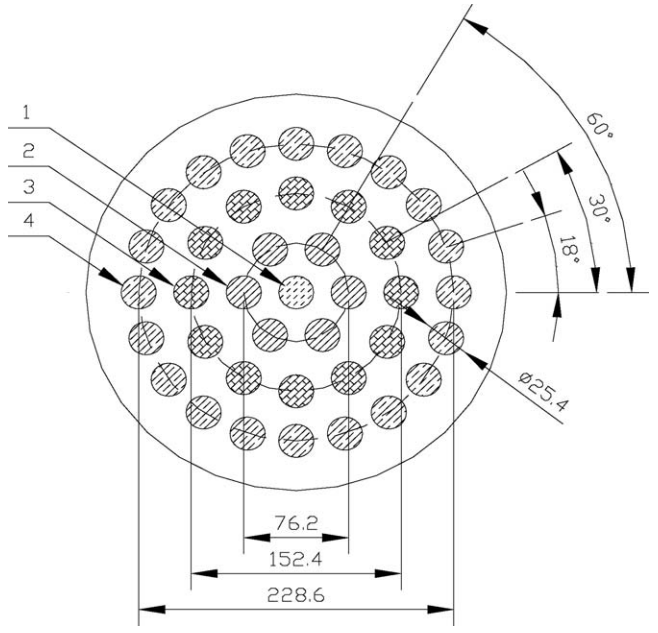

Fig. 2. Schematic diagram of the tube arrangement in the liquid collector: (1) center section with 1 tube; (2) inner section I with 6 tubes; (3) inner section II with 12 tubes; (4) outer section with 20 tubes (dimension unit: mm).

Table 1
The characteristics of the liquid distributors

Liquid distributor type	Number of nozzles	Nozzle diameter (mm)	Number of nozzles per unit area (m^{-2})
Single point type (SLD)	1	23.8	14
Cross-type (CLD)	16	4.8	219
Ladder type (LLD)	34	4.0	466

at the packing support level and collected in a separate container so that it did not interfere with the local liquid flow through the packing to the liquid collector described above.

For both liquid distribution and mass transfer coefficient measurements, three types of liquid distributors were used: single point (SLD), cross (CLD), and ladder type (LLD) distributors. The properties of these liquid distributors are shown in Table 1. The sketches of the distributor lay-outs are given in Fig. 3a–c.

2.2. Liquid distribution factor

Liquid maldistribution factors (indices) reported in the literature often represent only the deviation of the measured values from their own average. This may not show the deviation from an ideal state (uniform liquid flow distribution in a packed bed) when all liquid exiting the column is not collected or the wall flow is lumped into the flow in the bulk region of the packing. Ideally uniform liquid distribution at a given packing height of a column is only achieved when the ratios of the flow rate to the surface area of individual collecting cell not only are identical for all collecting cells across the column but also are the same and equal to the ratio of the inlet liquid flow rate to the entire cross-sectional area of the column. This can be expressed as

$$\frac{L_1}{A_2} = \frac{L_2}{A_2} = \cdots = \frac{L_n}{A_n} = \frac{L}{A} \tag{4}$$

Therefore, a new liquid distribution index, D_L, which represents the level of uniformity of liquid distribution in a packed column, is proposed and defined as the root mean square deviation of individual values L_i/A_i from the overall averaged value L/A:

$$D_L = \frac{1}{n}\sqrt{\sum_{i=1}^{n}\left(1 - \frac{L_i/A_i}{L/A}\right)^2} \tag{5}$$

The value of D_L is always positive and a value of zero indicates ideal liquid distribution, i.e. perfectly uniform liquid distribution. The larger the value of D_L, the less uniform the liquid flow distribution is. The value of D_L evaluated from Eq. (5) represents the deviation of measured values from an ideally perfect uniformity of liquid flow distribution in a packed bed.

2.3. Mass transfer coefficient measurement

The electrochemical limiting diffusion-current technique (LDCT) was used to measure the local mass transfer coefficient. Local mass transfer coefficients were measured at 81 locations over nine axial levels. At each axial level, nine electrodes

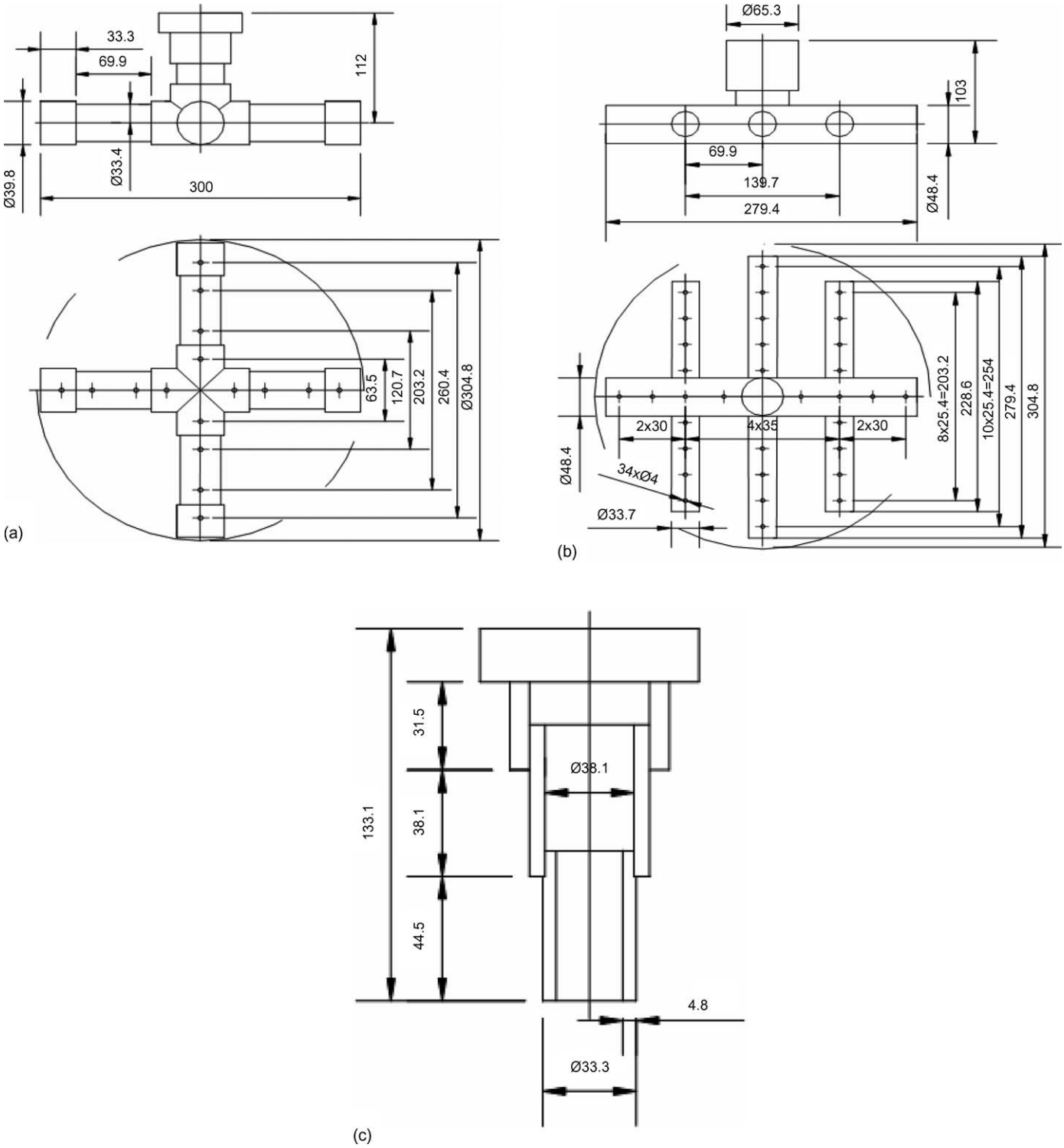

Fig. 3. (a) Side view (top) and lay-out (bottom) of cross-type liquid distributor (CLD). All dimensions are in millimeter. (b) Side view (top) and lay-out (bottom) of ladder-type liquid distributor (LLD). All dimensions are in millimeter. (c) Lay-out of single-point liquid distributor (SLD). All dimensions are in millimeter.

were arranged at three radial positions as shown in Fig. 4. The axial levels used in the experiments are equivalent to the ratios of the axial distance from the top of the bed to the column diameter, x/D, of 0.5, 1.0, 2.0, 2.5, 3.0, 3.5, 4.0, 5.0 and 5.5. Ferricyanide/ferrocyanide redox couple was selected as the reaction system with a large excess of sodium hydroxide as a supporting electrolyte to reduce the effect of ionic migration. In the present study, the concentrations of ferricyanide, ferrocyanide and sodium hydroxide used were 3.6, 4.0, and 500 mol m^{-3}, respectively.

The limiting current (i_L) obtained from the voltage drop over a known resistor is proportional to the liquid-to-solid mass transfer

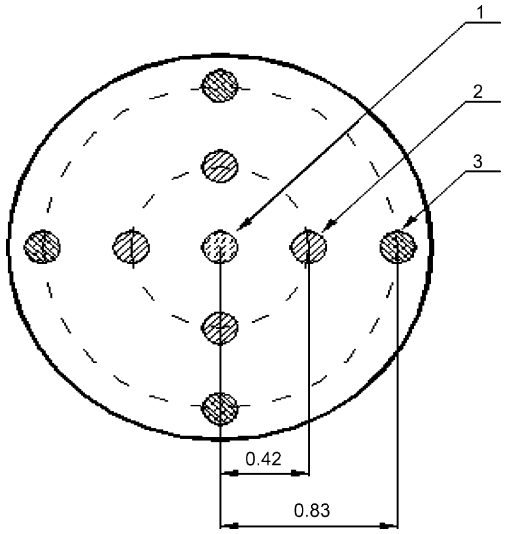

Fig. 4. Schematic diagram of the electrode arrangement in a layer: (1) central electrodes; (2) inner electrodes; (3) outer electrodes. The distance between centers of electrodes is shown in unit of *r*/*R*.

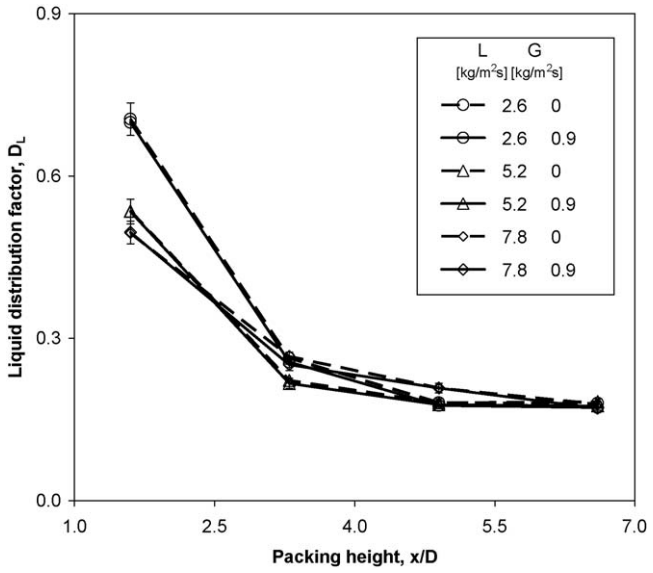

Fig. 5. Liquid distribution factor at different *x*/*D* levels for SLD.

coefficient ($k_{L–S}$) at the cathode surface (nickel-coated packing) as shown in the following equation:

$$k_{L–S} = \frac{i_L}{azFC_\infty} \quad (6)$$

where a is the surface area of the cathode, z the number of electrons transferred in the oxidation–reduction reaction, F the Faraday constant and C_∞ is the ferricyanide concentration in the bulk electrolyte.

The ferricyanide concentration in the electrolyte was determined by the iodometric method. Accordingly, the Schmidt number was around 1500. The details of the experimental apparatus and procedures are given elsewhere [15,20].

3. Results and discussion

3.1. Liquid distribution

Fig. 5 shows the liquid distribution factor for the single-point liquid distributor (SLD) at different *x*/*D* levels. Solid lines illustrate experimental data with a gas flow rate of 0.9 kg m^{-2} s^{-1} and dotted lines without a gas flow. For all inlet liquid flow rates, the overlapping of solid and dotted lines indicates that gas flow did not affect liquid distribution. It is relevant to note that the gas flow rate of 0.9 kg m^{-2} s^{-1} used in the present study is much lower than the loading point of 2.2 kg m^{-2} s^{-1} for air/water system, which is estimated by Robbins' pressure drop correlation [24]. The insignificant effect of the gas flow below loading point on the liquid distribution has been reported in the literature. Some of the more recent ones are those from Kouri and Sohlo [2] and Yin et al. [25], who pointed out that at low gas flow rates, the effect of the gas flow rate on liquid radial dispersion was insignificant. However, liquid radial mixing increased significantly at the gas flow rate above the loading point.

As can be seen in Fig. 5, at *x*/*D* of 1.6 the liquid distribution factor decreases drastically with increases in liquid flow rate, however, at larger *x*/*D* levels, the liquid distribution factors for all liquid flow rates (2.6, 5.2, and 7.8 kg m^{-2} s^{-1}) are comparable. Similar trends are also observed with CLD and LLD as shown in Fig. 6. This is in agreement with the results obtained by Hoek et al. [1] who reported that the maldistribution index did not vary considerably with liquid flow rate.

The initial liquid distribution at the top of the packed bed by the liquid distributor affected liquid flow distribution significantly. For SLD, the liquid distribution factor (D_L) decreased more than 45% when *x*/*D* increased from 1.6 to 3.3 at all liquid rates from 2.6 to 7.8 kg m^{-2} s^{-1}. This indicates that more development of the liquid flow occurred in the top section of the packed bed (equivalently lower *x*/*D*). However, for CLD and LLD the liquid distribution factor decreased to a lesser extent of about 28 and 15%, respectively, as can be seen in Fig. 6. With a larger number of nozzles per unit cross-section area of the column, CLD and LLD provided a more uniform initial liquid

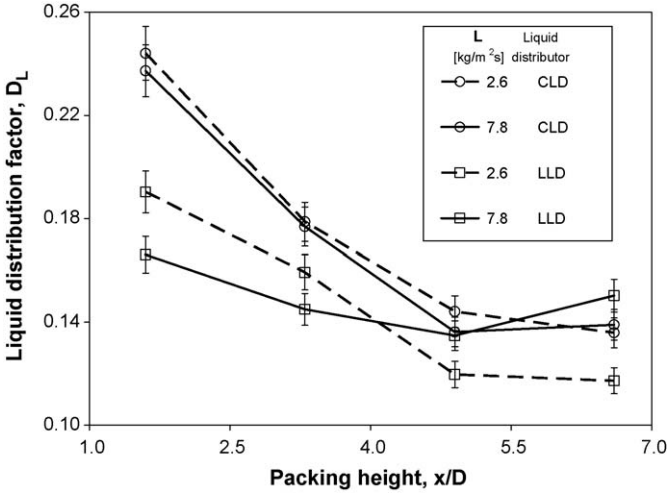

Fig. 6. Liquid distribution factor at different *x*/*D* levels for CLD and LLD (G = 0 kg m^{-2} s^{-1}).

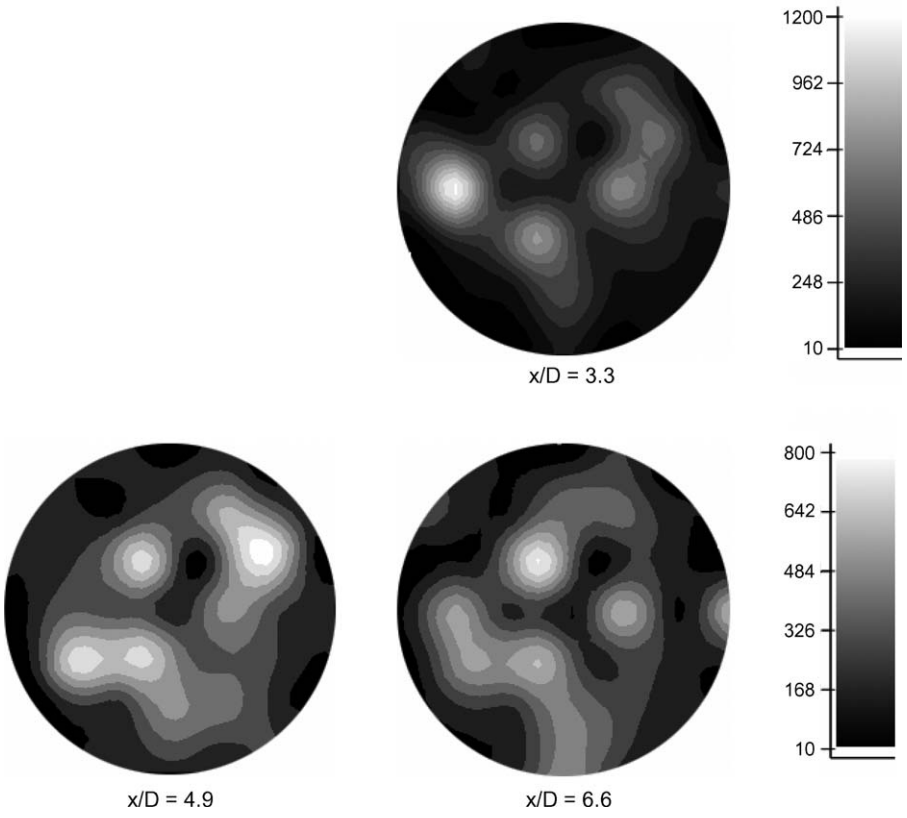

Fig. 7. Contour plots of local liquid flow rate (ml/min) at various x/D levels in the packed bed with CLD at $L = 7.8\,\mathrm{kg\,m^{-2}\,s}$ ($G = 0\,\mathrm{kg\,m^{-2}\,s^{-1}}$).

distribution, resulting in smaller changes in the liquid distribution factor along the packing height. Liquid flow distribution for SLD was much more sensitive to the bed height than for LLD due to a poor initial liquid distribution. Billet [26] also reported that liquid maldistribution decreased with increases in the number of liquid distributing points (nozzles).

For both CLD and LLD, it is noted that the initial decreasing trend of D_L with x/D is followed by an increasing trend of D_L starting at x/D of 4.9, especially at the higher liquid flow rate of $7.8\,\mathrm{kg\,m^{-2}\,s^{-1}}$, indicating the occurrence of liquid redistribution in the packed bed. The contour plots of the local liquid distribution at x/D of 3.3, 4.9 and 6.6 with CLD in Fig. 7 reconfirm the occurrence of liquid redistribution at x/D of 4.9. The more contrast on the contour plot indicates the larger difference in local liquid flow rates or less uniform liquid distribution in the bed. It can be seen in Fig. 7 that radial liquid distribution developed along the packing height. At x/D of 4.9 the liquid flow distribution is relatively uniform, as shown by a less color contrast of the contour plot, and then it slightly becomes less uniform at x/D of 6.6 indicating the occurrence of liquid redistribution. Liquid redistribution has been reported by several researchers, and redistributors were proposed to install at x/D within the range of 5–10 [27,28] or 3–10 [29] to improve the overall liquid distribution.

Liquid redistribution indicated by the relationship between D_L and x/D shows the advantage of the proposed liquid distribution factor over other reported factors in evaluating liquid flow distribution in a packed bed. For the same experimental data set, as an example, the values of the maldistribution factor were calculated from various equations and plotted in Figs. 8 and 9. Fig. 8 shows the variation of the maldistribution factor M_{f2} with the packing height at different inlet liquid flow rates. For a comparison of various maldistribution factors and D_L for the same data set, Fig. 9 shows the liquid maldistribution factors M_{f1}, M_{f2}, M_{f3}, and liquid distribution factor D_L, respectively. As can be seen in Figs. 8 and 9, the maldistribution factors M_{f1}, M_{f2}

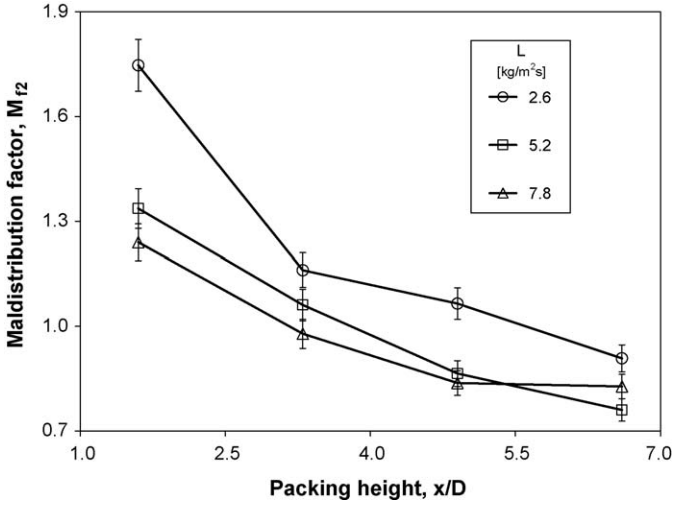

Fig. 8. Liquid maldistribution factor at different x/D levels for CLD and $G = 0\,\mathrm{kg\,m^{-2}\,s^{-1}}$.

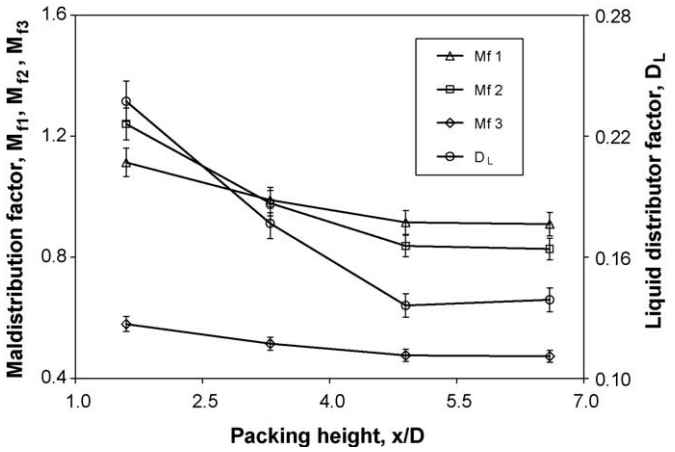

Fig. 9. Liquid maldistribution and distribution factor M_{f1}, M_{f2}, M_{f3}, D_L, defined in Eqs. (1)–(3) and (5), respectively, for CLD and $G = 0\,kg\,m^{-2}\,s^{-1}$, $L = 7.8\,kg\,m^{-2}\,s^{-1}$.

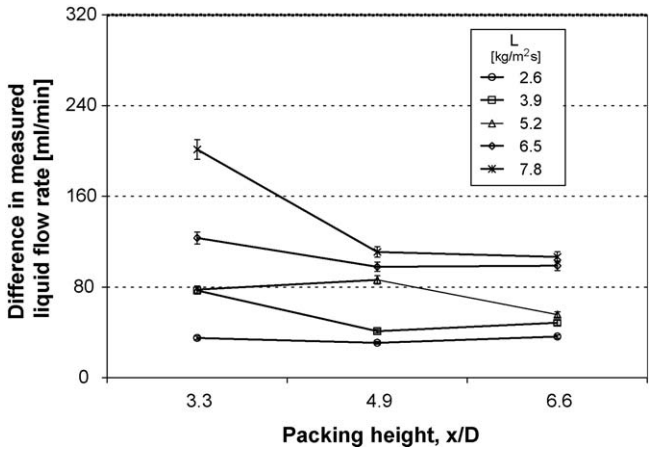

Fig. 11. The difference in measured liquid flow rate of two following x/D levels for CLD and $G = 0\,kg\,m^{-2}\,s^{-1}$.

and M_{f3} keep decreasing with the packing height beyond x/D of 4.9, except D_L, indicating that there would be further liquid distribution improvement. However, some deterioration of liquid distribution in fact was observed at $x/D > 4.9$ as previously shown in Figs. 6 and 7 and the increase of D_L shown in Fig. 9. In other words, these maldistribution factors failed to reveal the liquid redistribution in the bed.

In order to elucidate the flow development along the packed bed, the fluctuation of local liquid flow rate with the axial distance x/D was examined. The fluctuation is reflected through the change in the local liquid flow rate to a cell between two consecutive axial levels. When a fully developed flow is reached in the packed bed, the fluctuation in the local liquid flow rate with x/D would be non-significant, i.e. the change in the local liquid flow rate with x/D would level off and remain relatively constant, unless liquid redistribution occurs further down the column. The change of liquid flow rate to an individual liquid collecting cell was calculated from the liquid flow to the same cell at two consecutive axial levels. The arithmetic average of the values of the flow rate change for all 39 cells was then calculated. The averaged values obtained are plotted in Figs. 10–12 for SLD, CLD and LLD, respectively. In Figs. 10–12, a point at a certain x/D represents the averaged change of local liquid flow rate (to 39 cells in the liquid collector) over the cross-section of the column when the liquid flows from an upper x/D level to the specific x/D at which the data point is plotted, e.g. the value at $x/D = 3.3$ is for the change of the flow from $x/D = 1.6$ to 3.3.

Generally, for both SLD and CLD, the difference in the measured local liquid flow rate decreased with increases in x/D as can be seen in Figs. 10 and 11. The largest change in the liquid flow rate was at $x/D = 3.3$, which was the change in the liquid rate between x/D level of 1.6 and 3.3. The flow rate change became moderate for SLD and insignificant for CLD at $x/D = 4.9$ and beyond. This indicates that there existed flow development along the packing height with nearly full developed flow at $x/D \geq 4.9$. On the other hand, the difference in the measured local liquid flow rate for LLD remained relatively constant with x/D. However, at an inlet liquid flow rate of $7.8\,kg\,m^{-2}\,s^{-1}$ the flow rate change increased slightly at $x/D = 6.6$, indicating some deterioration of liquid distribution in the packed bed when liquid flowed from the axial level $x/D = 4.9$–6.6. In addition, from the measurements of the wall flow using a concentric ring with a gap of 12 mm from the inside wall of the column in the present study,

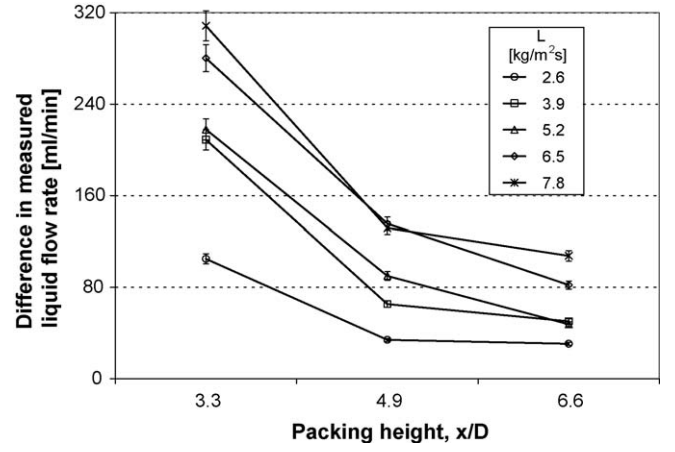

Fig. 10. The difference in measured liquid flow rate of two following x/D levels for SLD and $G = 0\,kg\,m^{-2}\,s^{-1}$.

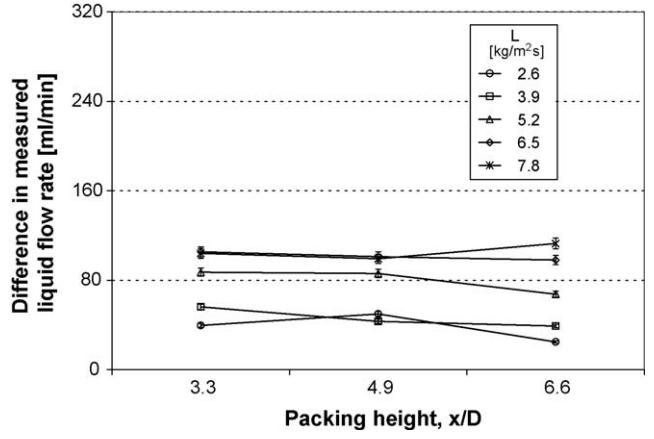

Fig. 12. The difference in measured liquid flow rate of two following x/D levels for LLD and $G = 0\,kg\,m^{-2}\,s^{-1}$.

fully developed wall flow was observed at $x/D = 4.9$ for LLD, which was about 5.5% of the total liquid flow rate to the bed. This implies that liquid redistribution from wall region back to the bulk region of the packed bed might occur at x/D level beyond 4.9. It is interesting to note that the liquid distribution factor, D_L, also increases at this x/D level as shown in Fig. 6, and some deterioration of the uniformity of local liquid velocity beyond $x/D = 4.9$ was observed in similar contour plots as of Fig. 7.

It was also noted that the change in the local liquid flow rate increased with the inlet liquid flow rate but decreased with the number of nozzles per unit area of the liquid distributor. At higher inlet liquid flow rates, more liquid channeling could occur within the opened structure of random Pall rings. In addition, at a higher liquid inlet flow rate, local liquid velocity or local flow rate was proportionally higher. Therefore, based on the order of magnitude of liquid flow in the packed bed, changes in the local liquid flow rate with x/D were higher although the percentage changes (i.e. normalized local flow rates against the inlet liquid flow rate) were relatively comparable. For SLD, the liquid flow entered the column at the central region in the top section of the packed bed, resulting in very high local liquid flow in the central region at $x/D = 1.6$. As the liquid flowed down the packed bed, it was spread out in the radial direction by the packing; hence, the local liquid flow rates became much smaller and more even over the cross-section of the column at $x/D = 3.3$. Therefore, the change in the local liquid flow rate between $x/D = 1.6$ and 3.3 was very high. For liquid distributors with a larger number of nozzles per unit cross-section area of the column (such as LLD), the flow development along the packing is small, due to better initial liquid distribution. Therefore, the change in the local liquid flow rate with x/D for LLD was smaller than those for CLD and SLD. At the inlet liquid flow rate of 7.8 kg m^{-2} s and the x/D level of 3.3, the change in the local liquid flow rate for LLD is two times smaller than that of CLD and three times smaller than that of SLD.

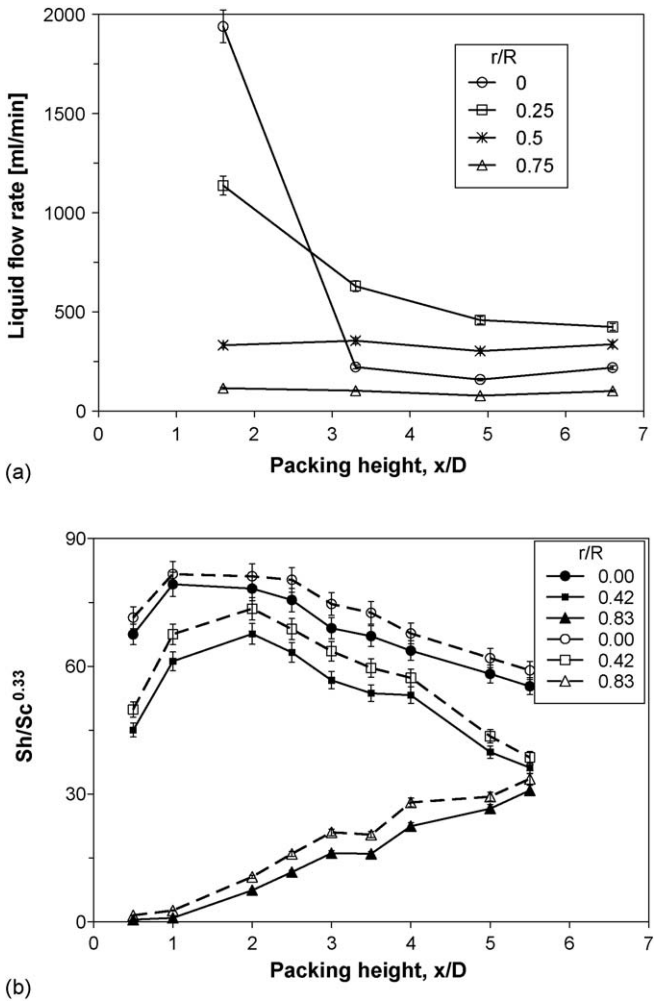

Fig. 13. Local liquid flow rate at $L = 6.5$ kg m^{-2} s^{-1} (a) and local mass transfer coefficient (b) vs. x/D level at different radial locations for SLD ($G = 0$ kg m^{-2} s^{-1}). The solid and dotted lines indicate the case for liquid rate, L, of 6.5 and 13.0 kg m^{-2} s^{-1}, respectively.

3.2. Effect of liquid flow distribution on the mass transfer coefficient

The effect of liquid distribution on the local mass transfer coefficient was evaluated. The local liquid flow rate and local mass transfer coefficients, expressed in terms of $Sh/Sc^{0.33}$, are plotted against the x/D level in Figs. 13–15. In Figs. 13a, 14a, and 15a each data point for the local liquid flow rate at a radial location (r/R) represents the arithmetic average of all measured points at that given radial location, i.e. the average of 1 point at the central section ($r/R = 0$), 6 points at the inner section I ($r/R = 0.25$), 12 points at the inner section II ($r/R = 0.50$), and 20 points at the outer section ($r/R = 0.75$) as shown in Fig. 2. Similarly, in Figs. 13b, 14b, and 15b each data point in the graphs of the outer ($r/R = 0.83$) and the inner ($r/R = 0.42$) sections represents the arithmetic average of all four electrodes at the given radial position. The value for the center section ($r/R = 0$) is the average for two electrodes shown as one at the central location in Fig. 4. Two electrodes were used for better representation of the central region of the bed.

For SLD, the highest local flow rate of liquid was at the central section close to the top of the packed bed (small x/D values) as shown in Fig. 13a. This correspondingly resulted in the highest local mass transfer coefficient (Fig. 13b). The single-point liquid distributor with only one central nozzle provided a poor initial liquid distribution. Close to the top of the packed bed, liquid stream concentrated in the central section of the column, resulting in high mass transfer in this section (Fig. 13b). Liquid spread out radially when it cascaded down the packed bed. Therefore, at deeper axial levels (higher x/D values) the local liquid velocity in the central section decreased, and hence, a reduction in the local mass transfer coefficient was observed. A similar trend was also observed for the inner section. On the other hand, along the packing height, the local mass transfer coefficient in the outer section increased due to liquid spreading from the central region to the outer section that was not wetted adequately in the upper part of the packed bed (low x/D levels). This variation pattern of the local liquid flow rate and mass transfer coefficient was also observed by Kouri and Sohlo [2], and Gostick et al. [20].

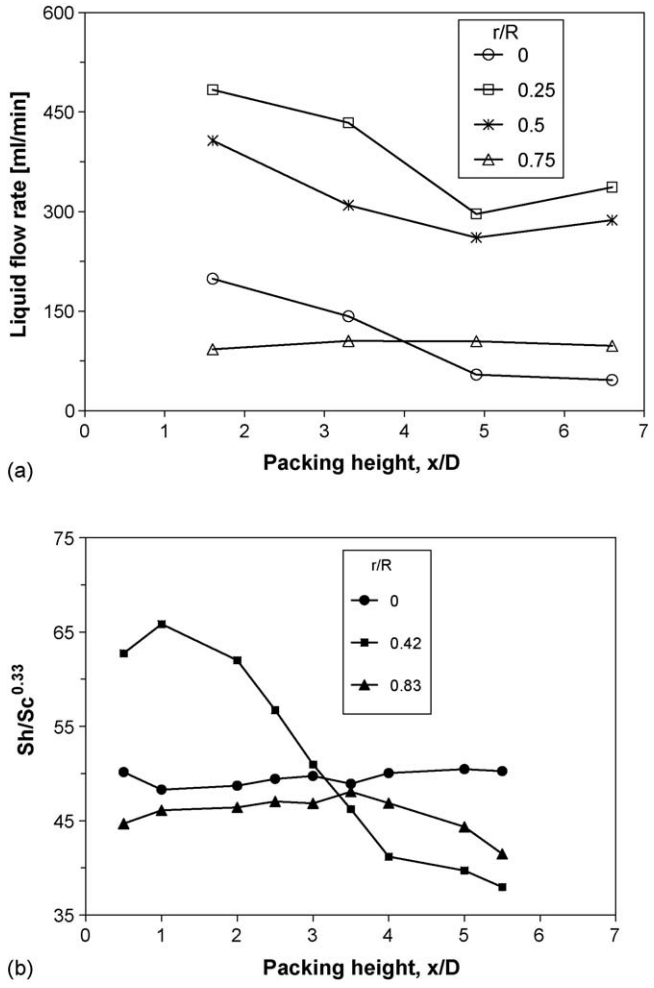

Fig. 14. Local liquid flow rate (a) and local mass transfer coefficient (b) vs. x/D level at different radial locations for CLD at $L = 6.5\,\mathrm{kg\,m^{-2}\,s^{-1}}$ ($G = 0\,\mathrm{kg\,m^{-2}\,s^{-1}}$).

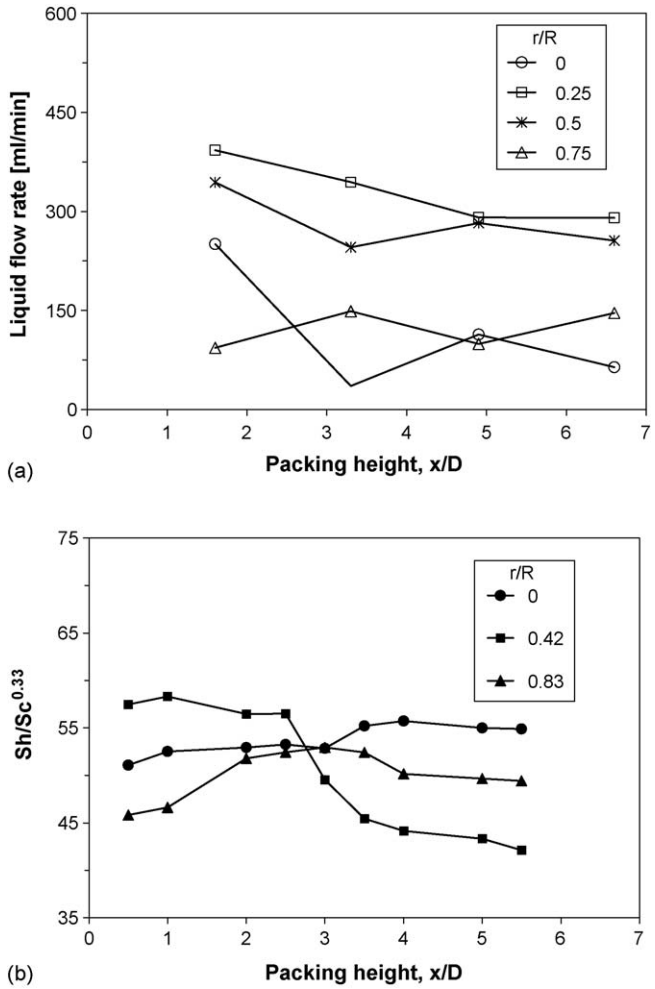

Fig. 15. Local liquid flow rate (a) and local mass transfer coefficient (b) vs. x/D level for LLD at $L = 6.5\,\mathrm{kg\,m^{-2}\,s^{-1}}$ ($G = 0\,\mathrm{kg\,m^{-2}\,s^{-1}}$).

For SLD, at all x/D levels the local mass transfer coefficient increased with the liquid flow rate as expected (Fig. 13b). Similar result was reported in literature [30]. In case of multi-point liquid distributors (CLD and LLD), the variation of the local liquid flow rate and the local mass transfer coefficient with the bed height was smaller than that with the single-point liquid distributor (Figs. 14 and 15). Multi-point liquid distributors, with larger numbers of nozzles per unit cross-sectional area of the column, provided a more uniform initial liquid distribution. Furthermore, as shown in Fig. 3a and b there was no nozzle at the center of these liquid distributors, hence, liquid flow from the distributor concentrated mostly at the inner region as shown in Figs. 14a and 15a. Therefore, local liquid flow rates at the inner sections with r/R of 0.25 and 0.50 were higher than those at the central and outer sections (Figs. 14a and 15a). The local mass transfer coefficient was correspondingly higher at the inner region ($x/D = 0.42$) due to higher liquid velocity. Similar radial profile of the mass transfer coefficient was reported in literature [31].

In case of a poor initial liquid distribution with SLD, the variation of the local liquid flow rate and the local mass transfer coefficient with locations in the packed bed was very large compared to that with a more uniform initial liquid distribution provided by CLD and LLD. For SLD, the difference between the maximum and minimum local liquid flow rate was over two and three times larger than those for CLD and LLD, respectively, and the difference between highest and lowest values of the local mass transfer coefficient was over five times larger than those for CLD and LLD.

3.3. Volume-averaged overall mass transfer coefficient

In order to obtain the overall mass transfer across the column, a correlation for the overall mass transfer coefficient (in terms of the Sherwood number) was developed taking into account the partial volumes of different radial and axial segments of the column where the measurement points were located. The estimated overall mass transfer coefficient from the local mass transfer coefficient would be more accurate because the variation of mass transfer with radial and axial location is incorporated into the model.

Fig. 16 shows the segmentation of the packed bed for the estimation of the partial volume (or volume factor) that is the

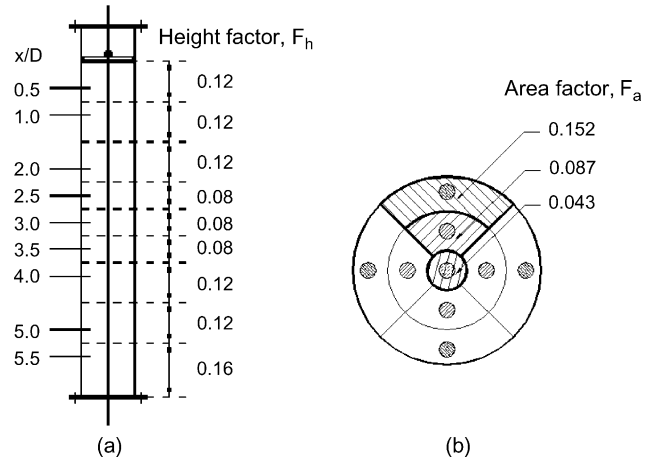

Fig. 16. Segmentation of the column for estimation of the local volume factor from the height and area factors.

product of the height and area factors. For the radial location effect, the local mass transfer coefficient was multiplied by the area factor F_a of the local area surrounding the measuring point. The area factor F_a is defined as the ratio of the local area to the cross-sectional area of the column. For the axial location effect the local mass transfer coefficient was again multiplied by the height factor F_h. The height factor F_h is defined as the ratio of the segment height to the overall packing height in the column. The values of the local mass transfer coefficient, weighed by the volume factor F_v ($F_v = F_a F_h$), were then used to determine the coefficients a and b in the relationship between the Sherwood number and the Reynolds number as below:

$$\frac{Sh}{Sc^{0.33}} = a\, Re^{b} \tag{9}$$

where Re is the particle Reynolds number, Sc the Schmidt number and Sh is the Sherwood number.

The variations of the overall mass transfer coefficient and the liquid distribution factor with the Reynolds number are plotted in Fig. 17. In this figure each data point for the liquid distribution factor represents the value calculated from the new liquid distribution factor described by Eq. (5) using all 156 measured points in the column at all 4 axial levels with 39 points at each level. As can be seen in Fig. 17, the mass transfer coefficient in the form of $Sh/Sc^{0.33}$ is proportional to the Reynolds number to a power of 0.26 for CLD and 0.44 for SLD, which is in the range of reported literature values. Furthermore, the effect of the Reynolds number on the mass transfer coefficient as well as the liquid distribution factor for CLD is less than the case with SLD as indicated by a lower exponent of the Reynolds number in the correlation. This can be attributed to better overall liquid distribution in the packed bed due to good initial liquid distribution provided by CLD. This is also reflected through an insignificant variation of D_L with the Reynolds number for CLD. On the other hand, liquid distribution with SLD was enhanced significantly with increases in the liquid flow rate, i.e. Re values, especially at the low end of the liquid flow rate range where higher liquid flow rates help spreading liquid out more in the radial direction in the packed bed.

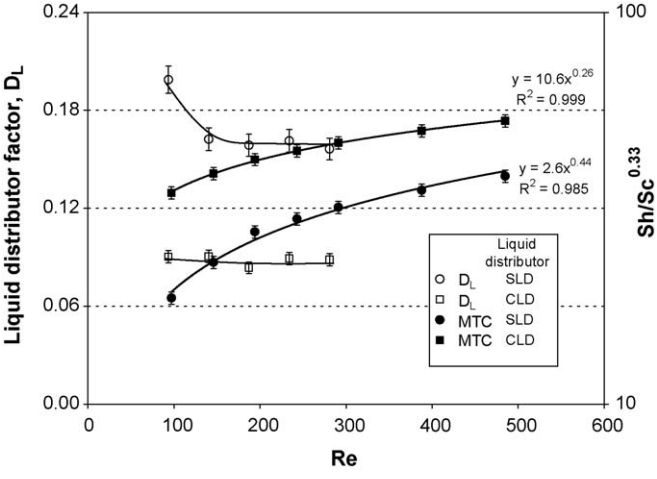

Fig. 17. Relationship of the overall mass transfer coefficient (MTC) and liquid distribution factor with the particle Reynolds number.

4. Conclusions

From the results obtained in the present study, it can be concluded that:

- Liquid distribution affected mass transfer significantly. The variation of liquid distribution in the column was reflected by the variation of the local mass transfer coefficient.
- Gas flow rate below the loading point did not have a noticeable effect on liquid distribution.
- The design of the liquid distributor is critical for liquid distribution and mass transfer in a random packed column. Liquid distribution and the local mass transfer coefficient with SLD were more sensitive to the bed height than those for CLD and LLD, due to the poor initial liquid distribution provided by SLD.
- A correlation of the overall mass transfer with the particle Reynolds number was developed using the local volume segments of different radial and axial locations in the column. The mass transfer coefficient was found to be proportional to the Reynolds number to a power of about 0.26 for CLD and 0.44 for SLD.
- A new liquid distribution factor for evaluation of liquid distribution in a packed column was introduced. The advantage of the proposed factor is that it presents the deviation of the local liquid flow rate from a perfectly uniform liquid distribution, considering the area of the cross-section of the collecting cell. This makes the proposed factor applicable to any liquid collecting system, independent to the number and the shape of the collecting cells. In addition, the new liquid distribution factor appeared to be able to reveal the occurrence of liquid redistribution in the packed bed.

Acknowledgement

Financial support from the Natural Sciences and Engineering Research Council of Canada (NSERC) to this project is greatly appreciated.

References

[1] P.J. Hoek, A. Wesselingh, F.J. Zuiderweg, Small scale and large scale liquid maldistribution in packed columns, Chem. Eng. Res. Des. 64 (1986) 431–449.

[2] R.J. Kouri, J. Sohlo, Liquid and gas flow patterns in random packings, Chem. Eng. J. 61 (1996) 95–105.

[3] R. Macias-Salinas, J.R. Fair, Axial mixing in modern packings, gas and liquid phases. I. Single-phase flow, AIChE J. 45 (1999) 222–239.

[4] V.J. Inglezakis, M. Lemonidou, H.P. Grigoropoulou, Liquid holdup and flow dispersion in zeolite packed beds, Chem. Eng. Sci. 56 (2001) 5049–5057.

[5] N.A. Tsochatzidis, A.J. Karabelas, D. Giakoumakis, G.A. Huff, An investigation of liquid maldistribution in trickle beds, Chem. Eng. Sci. 57 (2002) 3543–3555.

[6] N.A. Tsochatzidia, A.J. Karabelas, M. Kostoglou, A.J. Karabelas, A conductance probe for measuring liquid fraction in pipes and packed beds, Int. J. Multiphase Flow 18 (1992) 653–667.

[7] T. Loser, G. Petritsch, D. Mewes, Investigation of the two-phase countercurrent flow in structured packings using capacitance tomography, in: Proceedings of the First World Congress on Industrial Process Tomography, Buxtion, Greater Manchester, 14–17 April, 1999, pp. 354–361.

[8] N. Reinecke, D. Mewes, Investigation of the two-phase flow in trickle-bed reactors using capacitance tomography, Chem. Eng. Sci. 52 (1997) 2111–2127.

[9] F. Yin, A. Afacan, K. Nandakumar, K.T. Chuang, Liquid holdup distribution in packed columns: gamma ray tomography and CFD simulation, Chem. Eng. Proc. 41 (2002) 473–483.

[10] H.C. Groenhof, Scaling-up of packed columns. Part II, Chem. Eng. J. 14 (1977) 193–203.

[11] V. Stanek, N. Kolev, A study of the dependence of radial spread of liquid in random beds on local conditions of irrigation, Chem. Eng. Sci. 33 (1978) 1049–1053.

[12] M.M. Farid, D.J. Gunn, Liquid distribution and redistribution in packed columns. II. Experimental, Chem. Eng. Sci. 33 (1978) 1221–1231.

[13] B. Kunjummen, T.S. Prasad, P.S.T. Sai, Radial liquid distribution in gas-liquid concurrent downflow through packed beds, Bioproc. Eng. 22 (2000) 471–475.

[14] F.H. Yin, A. Afacan, K. Nandakumar, K.T. Chuang, CFD simulation and experimental study of liquid dispersion in randomly packed metal pall rings, Trans IChemE 80 (A) (2002) 135–144.

[15] Y. Zhu, H.D. Doan, A. Lohi, Relation of liquid distribution and local mass transfer coefficient in a packed bed, in: Proceedings of the Seventh World Congress of Chemical Engineering, Glasgow, UK, 2005.

[16] R.A. Al-Samadi, C.M. Evan, G.M. Cameron, M.E. Fayed, M. Leva, A study of liquid distribution in an industrial scale packed tower, in: AIChE Meeting, Houston, TX, April 1989.

[17] G. Guo, K.E. Thompson, Experimental analysis of local mass transfer in packed beds, Chem. Eng. Sci. 56 (2001) 121–132.

[18] S. Kumar, S.N. Upadhyay, V.K. Mathur, Low Reynolds number mass transfer in packed beds of cylindrical particles, Ind. Eng. Chem. Process Des. Dev. 16 (1977) 1–8.

[19] G.H. Sedahmed, A.M. El-Kayar, H.A. Farag, S.A. Noseir, Liquid solid mass transfer in packed beds of Raschig rings with upward two-phase (gas–liquid) flow, Chem. Eng. J. 62 (1996) 61–65.

[20] J. Gostick, H.D. Doan, A. Lohi, M. Pritzker, Investigation of local mass transfer in a packed bed using a limiting current technique, Ind. Eng. Chem. Res. 42 (2002) 3626–3634.

[21] T. Dang-Vu, H.D. Doan, A. Lohi, Local mass transfer in a packed bed: experiments and model, Ind. Eng. Chem. Res. 45 (2006) 1097–1104.

[22] A. Aroonwilas, A. Chakma, P. Tontiwachwuthikul, A. Veawab, Mathematical modeling of mass transfer and hydrodynamics in CO_2 absorbers packed with structured packings, Chem. Eng. Sci. 58 (2003) 4037–4053.

[23] V. Linek, T. Moucha, F.J. Rejl, Hydraulic and mass transfer characteristics of packings for absorption and distillation columns. Rauschert-Metal-Sattel-Rings, Trans IChemE 79 (A) (2001) 725–732.

[24] L.A. Robbins, Improve pressure drop prediction with a new correlation, Chem. Eng. Progr. 87 (1991) 87–91.

[25] F.H. Yin, Z. Wang, A. Afacan, K. Nandakumar, K.T. Chuang, Experimental studies of liquid flow maldistribution in a random packed bed, Can. J. Chem. Eng. 78 (2000) 449–457.

[26] R. Billet, Packed Towers in Processing and Environmental Technology, 1st ed., VCH Publisher, Inc., New York, 1995, p. 382.

[27] J.S. Eckert, in: P.A. Schweitzer (Ed.), Design of Packed Columns, Handbook of Separation Techniques for Chemical Engineers, McGraw-Hill, New York, 1997.

[28] R.F. Striggle Jr., Random Packings and Packed Towers, Gulf Publishing, Houston, TX, 1987.

[29] R.E. Treybal, Mass Transfer Operation, 3rd ed., McGraw-Hill, USA, 1995, p. 193.

[30] J. Levec, A. Lakota, Liquid–solid mass transfer in packed beds with concurrent downward two-phase flow, in: M. Quintard, M. Todorovic (Eds.), Heat and Mass Transfer in Porous Media, 1992, pp. 663–672.

[31] J.F. Gabitto, N.O. Lemcoff, Local solid–liquid mass transfer coefficient in a trickle bed reactor, Chem. Eng. J. 35 (1987) 69.